JOURNAL OF MATERIALS SCIENCE 27 (1992) 3743–3748

Effect of additive-oxide amount on sintering of Si_3N_4 with Y_2O_3 and Nd_2O_3

NAOTO HIROSAKI, AKIRA OKADA
Central Engineering Laboratories, Nissan Motor Co. Ltd, 1, Natsushima-cho, Yokosuka, 237 Japan

The effect of additive amount on the gas-pressure sintering of silicon nitride is investigated. Silicon nitride containing 0.5 to 10 mol% (SN10) of equimolar Y_2O_3–Nd_2O_3 is fired at 1600 to 1900 °C for 4 h in 10 MPa N_2 gas. A small amount of oxide (1 mol%; SN1) is effective for densification as well as a larger amount of oxide (6–10 mol%) when fired at 1900 °C. Composition analysis of sintered specimens indicates that SN1 densifies through a small amount of SiO_2-rich liquid-phase, whereas SN10 densifies by way of a large amount of additive-oxide-rich liquid phase.

1. Introduction

Sintered silicon nitride has been used for turbocharger rotors in recent years because of its favourable high-temperature characteristics, good mechanical properties and light weight [1, 2]. This material is currently used, however, only for applications at temperatures below 1000 °C because its strength is reduced at higher temperatures. The mechanical properties at elevated temperatures must be further improved if the material is to be used in higher-temperature engines such as the gas turbine engine.

Degradation of the high-temperature mechanical properties of silicon nitride is generally caused by grain-boundary phase softening. Dense, high-strength silicon nitride is fabricated using additive oxides and/or the effects of the mechanical force because the predominantly covalent Si–N bonding prohibits densification by classical solid-state sintering. Additive oxides react during firing with the layer of silica present around the raw silicon nitride powder to form a low-viscosity liquid phase, which promotes liquid-phase sintering [3]. The addition of oxides, however, has a negative effect on the high-temperature strength of sintered materials because the additives remain in a grain-boundary glass phase [4]. Thus a smaller amount of oxide additive is preferable as long as high density is achieved.

With the aim of decreasing the amount of additive, several experiments [5, 6] have been performed by hot-pressing (HP) or hot isostatic pressing (HIP). Using these methods, silicon nitride even without an additive oxide can densify up to near the theoretical density [5, 6]. These stress-assisted sintering methods, however, are expensive to use in mass-production systems.

Preliminary studies [7, 8] have already reported that silicon nitride containing 1 mol% rare-earth oxide additive can be effectively densified using the gas pressure sintering (GPS) method. The GPS method permits firing at higher temperatures than pressureless sintering because high-pressure nitrogen gas suppresses the thermal decomposition of silicon nitride [9], thus promoting sintering. Moreover this method can be employed for mass-production systems. The present study investigates the sintering behaviour of silicon nitride containing a small amount (1 mol%) and a large amount (10 mol%) of equimolar Y_2O_3–Nd_2O_3 additive and examines the microstructure of the sintered material.

2. Experimental procedure

The raw materials were Si_3N_4 powder (Grade H1, H. C. Starck) made by nitridation of Si, Y_2O_3 and Nd_2O_3 powder (99.9% pure, Shin-etsu Chemical). The Si_3N_4 powder was fine and pure as shown in Table I. The Si_3N_4 and 0.5 to 10 mol % of an equimolar ratio of Y_2O_3–Nd_2O_3 were ball-milled in ethanol for 94 h in a nylon jar, using sintered silicon nitride grinding media. The mixture compositions are shown in Table II. Theoretical density values calculated as the average of the raw-material values are also shown. The preliminary experimental results revealed a pick-up content from the grinding media of ≈ 0.2 wt %; oxide contamination from the grinding balls would thus be ≈ 0.02 wt % because sintered silicon nitride usually contains ≈ 10 wt % oxide additives. After the

TABLE I Powder characteristics of Si_3N_4

Impurity	Content (%)
C	0.43
O	1.37
Fe	0.006
Al	0.0054
Ca	0.006
Average particle size	0.6 μm
α-Si_3N_4 content	94%

0022–2461

TABLE II Mixture compositions

Sample	Composition (mol %)			Composition (wt %)			Theoretical density ($g\,cm^{-3}$)
	Si_3N_4	Y_2O_3	Nd_2O_3	Si_3N_4	Y_2O_3	Nd_2O_3	
SN10	90	5	5	81.8	7.3	10.9	3.49
SN6	94	3	3	88.8	4.5	6.7	3.37
SN2	98	1	1	96	1.6	2.4	3.25
SN1	99	0.5	0.5	98	0.8	1.2	3.22
SN05	99.5	0.25	0.25	99	0.4	0.6	3.21

powder mixtures were dried, they were die-pressed under 20 MPa and then isostatically pressed under 200 MPa; the resultant pressed specimens were about 5 mm × 6 mm × 50 mm.

Sintering was performed in a graphite resistance furnace. Pressed compacts were placed in a reaction-bonded silicon nitride crucible, which was put into the hot zone of a furnace. The specimens were fired at a constant heating rate of 500 °C h^{-1} and maintained at 1600 to 1900 °C for 4 h in 10 MPa N_2 gas. The densities of the sintered specimens were measured using the Archimedes method. The resulting products were identified by means of X-ray diffraction. The microstructures were investigated using fractured surfaces by a scanning electron microscope (SEM). Samples for observation under a transmission electron microscope (TEM) were prepared by diamond cutting, grinding, and polishing to a thickness of 50 μm, followed by ion-milling. The microstructure was observed by bright-field imaging in the TEM.

The oxygen content of the sintered material was determined using an oxygen–nitrogen analyser (System TC-436, Leco Corp.). A specimen was cut to a size of 3 mm × 4 mm × 0.5 mm with a diamond blade and heated in a vacuum at 800 °C for 1 h to remove water. After vacuum treatment the specimen was crushed. About 0.04 g of crushed specimen was placed in tin foil and set in a graphite crucible. The oxygen content was determined by CO_2 detection after fusion in a helium carrier gas.

The densification curve of the specimen during heating was measured using another graphite resistance furnace mounted with a dilatometer [10]. The specimens for dilatometric study were 10 mm in diameter and 12 mm in height. The compact was placed in a boron nitride crucible with a powder bed of Si_3N_4. The crucible was put into a carbon container serving as the susceptor for induction heating. The specimens were fired at a constant heating rate of 25 °C min^{-1} to 2000 °C in 1 MPa N_2; these conditions differed from those used for sintering because of the furnace design.

3. Results and discussion

3.1. Sintering behaviour

Fig. 1 shows the bulk density of silicon nitride containing 0.5 to 10 mol % of equimolar Y_2O_3–Nd_2O_3 fired at 1900 °C for 4 h, where the relative density was calculated assuming that the theoretical density was the average for the raw material. Two regions of additive content were found to be effective for sintering of Si_3N_4; a large-content region (6–10 mol %) and a low-content region (≈ 1 mol %). Silicon nitride containing 10 mol % of oxides (SN10) densified to 97% of theoretical density. The density decreased as the oxide additive content was lowered from 10 to 2 mol %. The material containing 2 mol % oxide (SN2) attained 91.7% of theoretical density. The material with 1 mol % oxide (SN1), however, reached 97.4% of theoretical density. The density decreased again to 78.8% of theoretical with 0.5 mol % of oxides (SN05). More than five furnace runs were carried out in this study and the same tendency was confirmed.

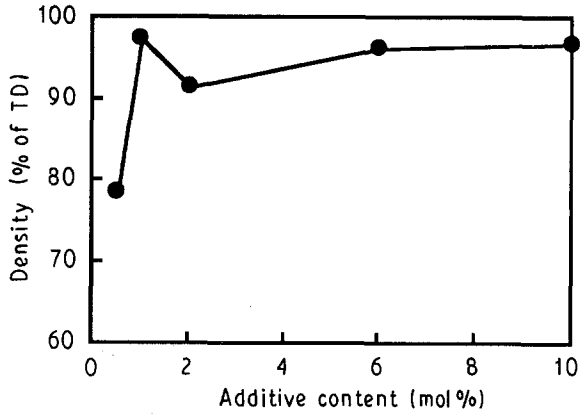

Figure 1 Density of Si_3N_4 containing 0.5–10 mol % of equimolar Y_2O_3–Nd_2O_3 fired at 1900 °C for 4 h in 10 MPa N_2.

Fig. 2 presents the sintering behaviour for SN1 and SN10 during firing at a constant heating rate of 25 °C min^{-1} up to 2000 °C. The shrinkage rates are also plotted in the figure. SN1 and SN10 had similar shrinkage curves, showing two densification processes. The first process (process I) started at 1600 °C and ended at 1850 °C; then the second (process II) started at 1900 °C. Mitomo and Mizuno [11] reported that Y_2O_3–Al_2O_3-doped Si_3N_4 densified by gas pressure sintering with two sintering processes; process I took place at < 1750 °C and process II at > 1750 °C. In the present study two densification processes were also observed and a high density was achieved using process II when fired at 1900 °C. SN1 and SN10 could not densify enough using only process I and needed process II for densification up to near the theoretical density.

Table III shows the results of X-ray diffraction analysis of silicon nitride containing 1 mol % (SN1) and 10 mol % (SN10) of oxide fired at 1600 to 1900 °C for 4 h. In all cases β-Si_3N_4 was observed, indicating

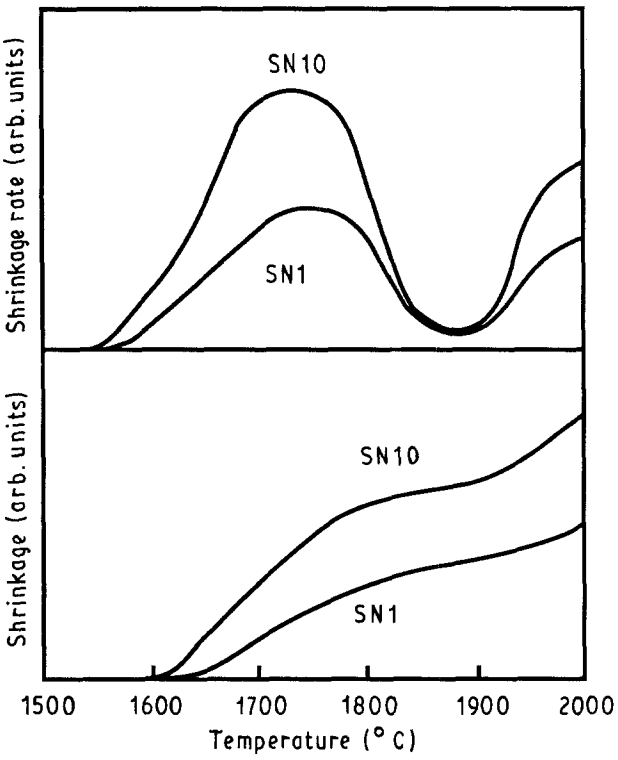

Figure 2 Sintering behaviour of silicon nitride with 10 mol % (SN10) and 1 mol % (SN1) of Y_2O_3–Nd_2O_3 fired at a constant heating rate of 25 °C min^{-1} up to 2000 °C in 1 MPa N_2.

that α to β transformation occurred at temperatures higher than 1600 °C. Besides β-Si_3N_4, α-Si_3N_4 was observed for SN1 sintered at 1600 °C. N-melilite ($Y_2Si_3O_3N_4$) was observed for SN10 sintered at 1600 to 1800 °C. These results agree with previous phase studies [12–14]. SN10 fired at 1900 °C, however, had no crystalline phase except β-Si_3N_4. This material had a liquid phase which solidified to a glass during cooling.

It has been reported that silicon nitride containing N-melilite oxidized at ≃ 1000 °C and caused the material to disintegrate [12] because oxidation increases the volume and creates surface stress which leads to cracking. Thus large amounts of N-melilite phase in SN10 are not desirable for oxidation. SN1 showed excellent oxidation resistance at 1200 to 1350 °C compared with SN10 [15].

Silicon nitride containing oxide additives is generally sintered by a liquid-phase sintering mechanism, and shrinkage begins with the formation of the liquid phase. The densification curves in Fig. 2 suggest that liquid formed near 1600 °C. Phase diagrams for Si_3N_4–SiO_2–Y_2O_3 [14] and Si_3N_4–SiO_2–Nd_2O_3 [16] suggest that this liquid is the SiO_2-rich composition in the system Si_3N_4–Y_2O_3–Nd_2O_3, which has the lowest formation temperature [17]. Densification via rearrangement and dissolution–reprecipitation started upon formation of this liquid. X-ray diffraction data indicates that α to β transformation occurred using this liquid. SN10 produced more liquid than SN1, resulting in the difference in shrinkage at 1600 °C. At the beginning of shrinkage (≃ 1600 °C) the liquid region was small, so that shrinkage occurred slowly. As the temperature rose, the amount of liquid increased with the increasing liquid-formation area, and further shrinkage was promoted. At 1900 °C, a second stage of shrinkage began. Using this liquid, SN1 and SN10 were densified up to near the theoretical density.

Fig. 3 shows the weight loss of silicon nitride with additive oxide during firing at 1900 °C for 4 h. The weight loss increased with decreasing additive amount; SN10 lost 1.2% and SN05 lost 3.5%. Weight loss is caused by thermal decomposition of silicon nitride and oxide. When Si_3N_4 with Y_2O_3–Nd_2O_3 is fired at high temperatures, several reactions can occur [18–20].

$$Si_3N_4(s) \rightarrow 3Si(l) + 2N_2(g) \quad (1)$$

$$Si_3N_4(s) \rightarrow 3Si(g) + 2N_2(g) \quad (2)$$

$$Si_3N_4(s) + 3SiO_2(s,l) \rightarrow 6SiO(g) + 2N_2(g) \quad (3)$$

$$Si_3N_4(s) + Y_2O_3(s) \rightarrow 3SiO(g) + N_2(g) + 2YN(s) \quad (4)$$

$$Si_3N_4(s) + Nd_2O_3(s) \rightarrow 3SiO(g) + N_2(g) + 2NdN(s) \quad (5)$$

Preliminary work [21] has already discussed the thermal decomposition of this system. Thermodynamic analysis suggested that the vapour pressure of Si(g) for Reaction 2 was 1 Pa and that of SiO(g) for Reactions 3 and 4 was 2×10^4 and 1×10^2 Pa, respectively, at 1900 °C in 10 MPa N_2. Reaction 5 was actually as non-reactive as Reaction 4 because the rare-earth elements involved had similar chemical properties. Successful sintering of Si_3N_4 containing a rare-earth oxide [22] has also suggested that Reactions 4 and 5

TABLE III X-ray diffraction data for Si_3N_4 with 1 and 10 mol % of Y_2O_3–Nd_2O_3 fired at 1600 to 1900 °C

Sintering temperature (°C)	XRD data 1 mol % additive	10 mol % additive
1600	α (s), β (s)	β (s), N-melilite (m)
1700	β (s)	β (s), N-melilite (m)
1800	β (s)	β (s), N-melilite (m)
1900	β (s)	β (s)

α: α-Si_3N_4, β: β-Si_3N_4, N-melilite: $Y_2Si_3O_3N_4$.

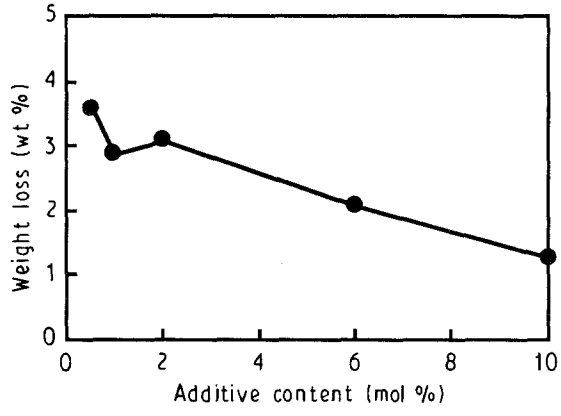

Figure 3 Weight loss of Si_3N_4 containing 0.5–10 mol % of equimolar Y_2O_3–Nd_2O_3 fired at 1900 °C for 4 h in 10 MPa N_2.

TABLE IV Oxygen content in the sintered material

Sample	Measured oxygen content (wt %)	Oxygen content in additive (wt %)
SN10	4.5	3.1
SN6	2.8	1.9
SN2	1.24	0.68
SN1	0.89	0.34
SN05	0.63	0.17

are stable, although a large weight loss was observed in sintering the Si_3N_4–SiO_2 system [23]. It was surmised that oxygen loss mainly occurred as a result of the reaction between silicon nitride and native silica, i.e. Reaction 3.

The material containing a low amount of additive would be more porous at higher temperatures than that containing larger amounts. Thus, weight loss increased as the additive oxide decreased because thermal decomposition reactions were accelerated.

Table IV shows the measured oxygen content of sintered material containing 0.5 to 10 mol % of oxide additives. The oxygen content derived from Y_2O_3 and Nd_2O_3 is also shown. The raw material used in the present study contained 1.37 wt % of oxygen, in the form of SiO_2 on the surface of the silicon nitride particles. The oxygen content of the sintered material was less than the sum of the oxygen contents in raw silicon nitride powder and oxide additives, suggesting that oxygen had been removed during firing. This oxygen loss mainly occurred as a result of Reaction 3. This reaction reduces the SiO_2 content of the material and consequently changes the amount and composition of liquid.

To discuss the liquid amount and composition which promote sintering of Si_3N_4, the oxide composition of the sintered material was estimated. Fig. 4 shows SiO_2, Y_2O_3 and Nd_2O_3 content in the sintered material. The silica fraction in the oxide system, $SiO_2/(SiO_2 + Y_2O_3 + Nd_2O_3)$, is also shown in the figure. These data were calculated using the oxygen content data in Table IV, assuming that (i) Y_2O_3 and Nd_2O_3 were not volatilized [21], and (ii) the difference in oxygen content between the measured oxygen value and the additive oxygen content formed SiO_2. As the additive content was decreased, the total oxide in the material, $SiO_2 + Y_2O_3 + Nd_2O_3$, decreased, but the SiO_2 fraction in the oxide system increased. SN10 contained 16 mol % of oxide with a 40% SiO_2 fraction and SN1 contained 3.4 mol % of oxide with a 70% SiO_2 fraction. Assuming that oxide in the sintered material formed liquid which promoted sintering, SN1 densified through the 70% of SiO_2 liquid and SN10 through the 40% of SiO_2 liquid.

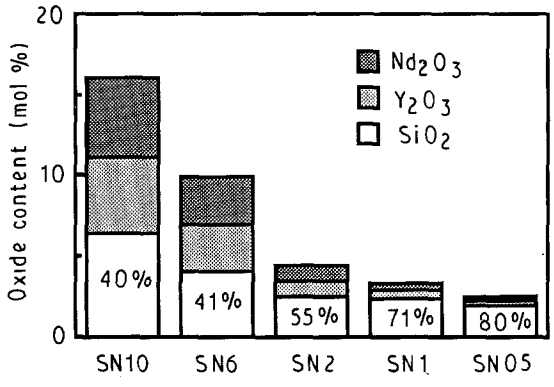

Figure 4 Oxide content in the sintered material and SiO_2 fraction in the oxide. These values were calculated using the data in Table IV.

The liquid composition is discussed here in terms of an Re_2O_3–SiO_2 (Re = Y and Nd) system using phase diagrams for Y_2O_3–SiO_2 and Nd_2O_3–SiO_2 [17], although the actual liquid composition which promotes sintering is an oxynitride, a system of Si–Y–Nd–O–N. These approximations should be reasonable because (i) phase diagrams for Si_3N_4–Re_2O_3–SiO_2 (Re = Y and Nd) [14, 16] show that the liquid composition is near the Re_2O_3–SiO_2 tie line and (ii) phase diagrams for Y_2O_3–SiO_2 and Nd_2O_3–SiO_2 are similar. The phase diagrams for Y_2O_3–SiO_2 and Nd_2O_3–SiO_2 [17] indicate that the liquid formation temperature differs with the ratio of Re_2O_3 to SiO_2. In the system SiO_2–Y_2O_3, liquid was produced at 1660 °C when the SiO_2 content exceeded 67%. On the other hand, a higher temperature was needed to form liquid when the SiO_2 content was below 67%: e.g. 1775 °C for 60 to 67% SiO_2, 1900 °C for 50 to 60% SiO_2, and 1800 °C for less than 50% SiO_2. The liquid-formation temperature in the system SiO_2–Nd_2O_3 showed a similar change according to the ratio of the SiO_2 content.

Phase diagrams account for the two regions of effective additive content. Fig. 4 indicates that SN10 contained 16 mol % of 40% SiO_2 oxide. Thus, SN10 densified through a large amount of liquid with a high melting temperature. When additive amounts were decreased, the liquid amount decreased and the liquid composition became SiO_2-rich. This decreased oxide content led to lowered sinterability. An increased SiO_2 fraction in the oxide lowered the sinterability in the range of 50 to 60%, but improved sinterability in the range $\geq$ 60%. Thus, SN1 was sintered by a smaller amount of liquid with a lower melting temperature than SN10. SN2 had an oxide whose SiO_2 fraction was 55%. The phase diagram suggests that this oxide composition produces a liquid with a high melting temperature. Thus, the density of SN2 decreased because the liquid had a high melting temperature.

3.2. Microstructure

Fig. 5 shows SEM photos of the fractured surface of silicon nitride containing 1 mol % of oxide fired at 1600, 1700 and 1900 °C. Equiaxed grains smaller than 1 μm were observed for the specimen fired at 1600 °C. The material fired at 1700 °C showed larger equiaxed grains. The material fired at 1900 °C, however, revealed abnormally elongated fibrous grains ($\approx$ 50 μm long) in addition to grains of $\approx$ 5 μm long. Such needle-like, large grains developed during process II in Fig. 2. Although hot-pressed silicon nitride without additive was reported to have uniform equi-axial

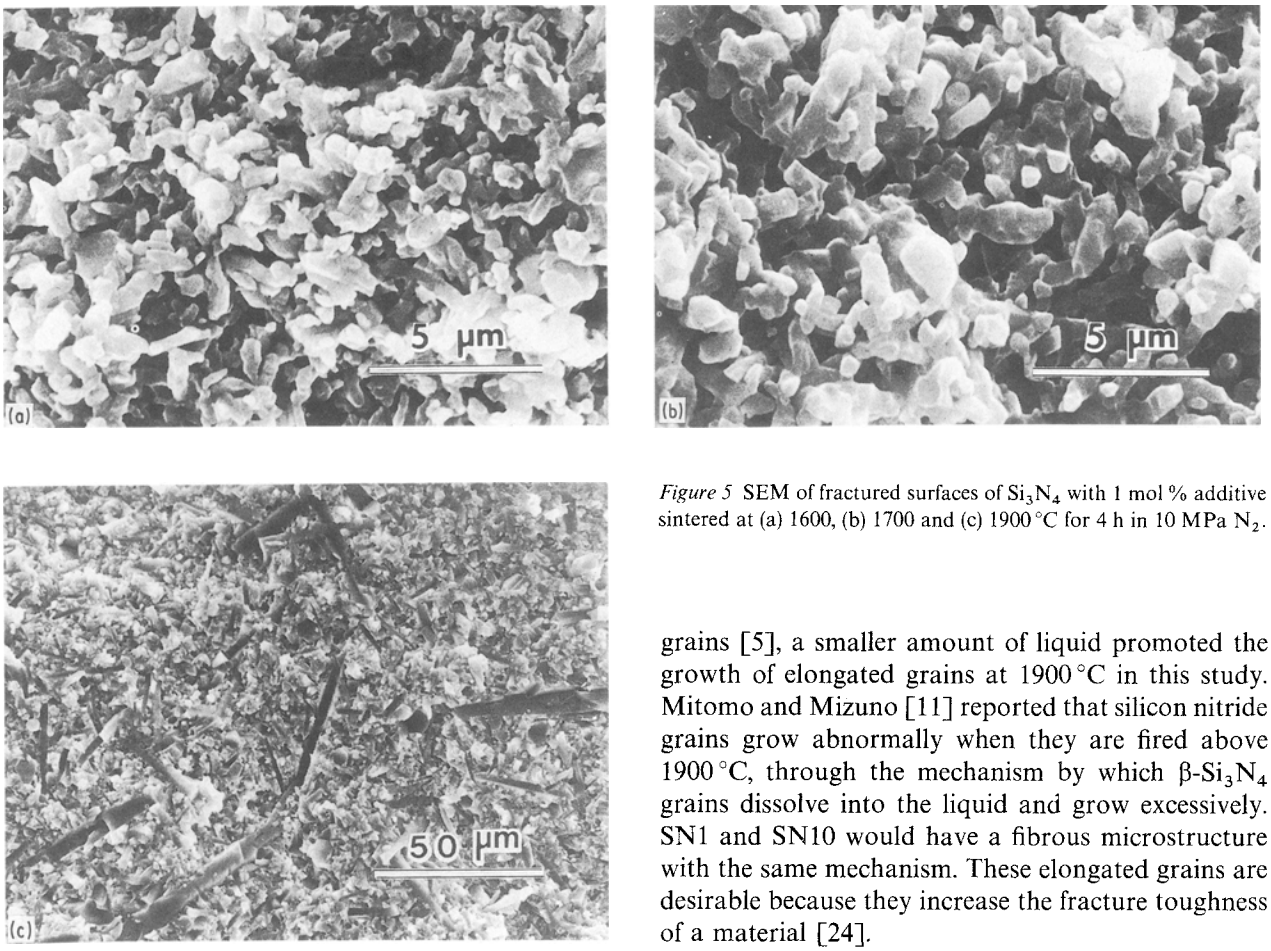

Figure 5 SEM of fractured surfaces of Si_3N_4 with 1 mol % additive sintered at (a) 1600, (b) 1700 and (c) 1900 °C for 4 h in 10 MPa N_2.

grains [5], a smaller amount of liquid promoted the growth of elongated grains at 1900 °C in this study. Mitomo and Mizuno [11] reported that silicon nitride grains grow abnormally when they are fired above 1900 °C, through the mechanism by which β-Si_3N_4 grains dissolve into the liquid and grow excessively. SN1 and SN10 would have a fibrous microstructure with the same mechanism. These elongated grains are desirable because they increase the fracture toughness of a material [24].

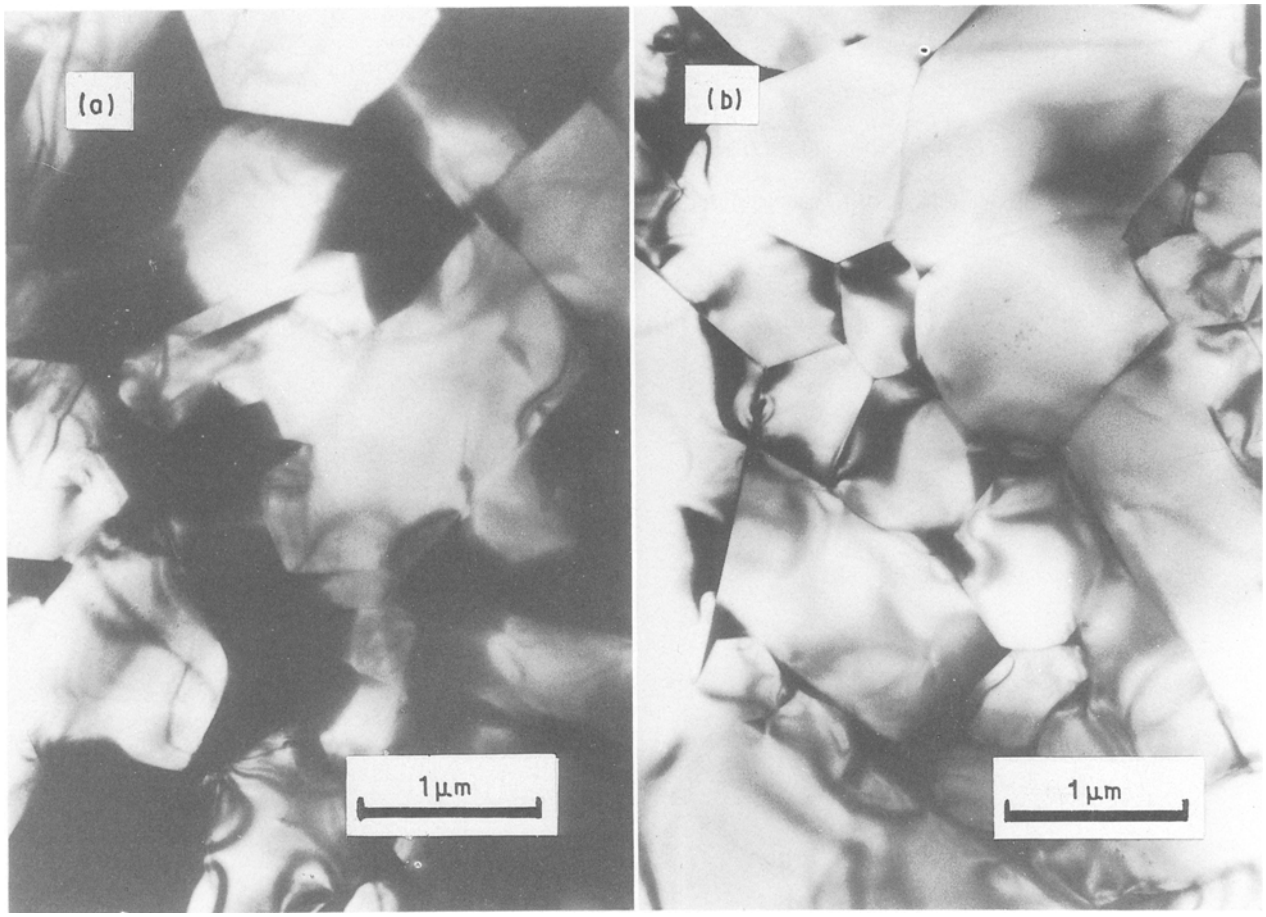

Figure 6 TEM of (a) Si_3N_4 with 10 mol % and (b) Si_3N_4 with 1 mol % of Y_2O_3–Nd_2O_3 sintered at 1900 °C for 4 h in 10 MPa N_2.

Fig. 6 shows bright-field TEM photos of SN1 (Fig. 6a) and SN10 (Fig. 6b). The β-Si_3N_4 grains were observed in light contrast, while grain boundary phases appear in darker contrast because of the greater electron absorption of Y and Nd which were concentrated in these phases. The Si_3N_4 grains of both specimens exhibited a similar size and shape but had different grain boundary features; the SN1 specimen contained a smaller amount of grain boundary phase than SN10. Less additive thus cause a smaller grain boundary phase.

4. Conclusions

1. 1 mol % of an equimolar Y_2O_3–Nd_2O_3 addition was effective for the densification of Si_3N_4 by gas-pressure sintering at 1900 °C for 4 h in 10 MPa N_2. This material (SN1) attained 97.4% of theoretical density.

2. The SN1 ceramic densified through an SiO_2-rich liquid phase, whereas silicon nitride with 10 mol % Y_2O_3–Nd_2O_3 (SN10) densified by way of an SiO_2-poor liquid phase.

3. The investigation of microstructures revealed that this material consisted of fibrous Si_3N_4 grains and a small amount of intergranular phase.

Acknowledgements

The authors want to thank Dr M. Mitomo for dilatometer measurements and for helpful discussions. Thanks are also due to Professor T. Iseki for permitting the use of the Leco apparatus.

References

1. K. KATAYAMA, T. WATANABE, K. MATOBA and N. KATOH, SAE Technical Paper Series 861 128 (1986).
2. K. MATOBA, K. KATAYAMA, M. KAWAMURA and T. MIZUNO, SAE Technical Paper Series 880 702 (1988).
3. G. R. TERWILLIGER and F. F. LANGE, *J. Amer. Ceram. Soc.* **57** (1974) 25.
4. D. RICHERSON, *Amer. Ceram. Soc. Bull.* **52** (1973) 560.
5. R. BECKER and F. THUMMLER, in "Energy and Ceramics", edited by P. Vincenzini (Elsevier, Amsterdam, 1980) p. 610.
6. Y. MIYAMOTO, K. TANAKA, M. SHIMADA and M. KOIZUMI, in "Ceramic Materials and Components for Engines", edited by W. Bunk and H. Hausner (German Ceramic Society, Bad Honnef, 1986) p. 271.
7. N. HIROSAKI and A. OKADA, *Seramikkusu Ronbunshi* **97** (1989) 637.
8. N. HIROSAKI, A. OKADA and Y. AKIMUNE, *J. Mater. Sci. Lett.* **9** (1990) 1322.
9. M. MITOMO, M. TSUTSUMI, E. BANNAI and T. TANAKA, *Amer. Ceram. Soc. Bull.* **55** (1976) 313.
10. M. MITOMO and K. MIZUNO, in "Ceramic Materials and Components for Engines", edited by W. Bunk and H. Hausner (German Ceramic Society, Bad Honnef, 1986) p. 263.
11. *Idem, Yogyo-Kyokai-Shi* **94** (1986) 96.
12. F. F. LANGE, S. C. SINGHAL and C. KUZNICKI, *J. Amer. Ceram. Soc.* **60** (1977) 249.
13. R. R. WILLS, S. HOLMQUIST, J. M. WIMMER and J. A. CUNNINGHAM, *J. Mater. Sci.* **11** (1976) 1305.
14. L. J. GAUCKLER, H. HOHNKE and T. Y. TIEN, *J. Amer. Ceram. Soc.* **63** (1980) 35.
15. N. HIROSAKI, Y. AKIMUNE, T. OGASAWARA and A. OKADA, *J. Mater. Sci. Lett.* **10** (1991) 753.
16. S. SLASOR, K. LIDDELL and D. P. THOMPSON, in "Special Ceramics 8", edited by S. P. Howlett and D. Taylor (Institute of Ceramics, Shelton, Stoke-on-Trent, UK, 1986) p. 51.
17. E. M. LEVIN, C. R. ROBBINS and H. F. McMURDIE, in "Phase Diagrams for Ceramists" (American Ceramic Society, Columbus, Ohio, 1969) Figs 2381 and 2388.
18. C. GRESKOVICH and S. PROCHAZKA, *J. Amer. Ceram. Soc.* **64** (1981) C96.
19. F. F. LANGE, *ibid.* **65** (1982) C120.
20. D. R. MESSIER and E. J. DEGUIRE, *ibid.* **67** (1984) 602.
21. N. HIROSAKI and A. OKADA, *ibid.* **72** (1989) 2359.
22. G. E. GAZZA, *Amer. Ceram. Soc. Bull.* **54** (1975) 778.
23. M. MITOMO, S. ONO, T. ASAMI and S. L. KANG, *Ceram. Int.* **15** (1989) 345.
24. F. F. LANGE, *J. Amer. Ceram. Soc.* **62** (1979) 428.

Received 12 March
and accepted 1 July 1991